1-1-2011

Evaluation of Toxicological Effects of Intra Tracheal Instilled CeO2 Nanoparticles on the Heart of Male Sprague-Dawley Rats

Radhakrishna Para
para@marshall.edu

Evaluation of toxicological effects of intra tracheal instilled CeO_2 nanoparticles on the heart of male Sprague-Dawley rats.

A thesis submitted to the

Graduate College of Marshall University

in partial fulfillment of the requirements for the degree of

Master of Science

Department of Biological Sciences

by

Radhakrishna Para

Approved by

Dr. Eric R. Blough, Committee Chairperson

Dr. David S. Mallory

Dr. Bin Wang

Marshall University

December 2011

ACKNOWLEDGEMENTS

First and foremost I would like to thank my mentor and guide Dr. Eric Blough for his invaluable suggestions and guidance throughout my master's program. I would have not made it to United States in the first place if he hadn't supported me. He has guided me at each step with lots of enthusiasm and motivated me when I needed it the most. I could not think of a better person or a mentor other than Eric. I am indebted to him for helping me achieve my master's degree in Biological Sciences. I would also like to thank my committee members Dr. David S. Mallory and Dr. Bin Wang for their detailed and constructive suggestions that helped me in writing my thesis. The support of my committee members has helped me in framing my thesis in a better way. I am also grateful to my lab mates Kevin, MiaZong, Sunil, Anjaiah, Paturi, Madhukar, Siva, Geeta, Ravi, Sudarsan, Prasanna, Hari, Thulluri and Sravanthi for helping in carrying out my experiments promptly. I owe my loving thanks to my wife Sai Prasanna, my daughter Harini and my parents who have lost a lot due to my research abroad. Nonetheless without their encouragement and support I would not have finished my thesis work.

Table of Contents

ABBREVIATIONS

AMPK	5' adenosine monophosphate-activated protein kinase
ANOVA	Analysis of variance on ranks
ATG	Autophagy related genes
Bax	Bcl-2 associated X protein
Bcl-2	B-cell lymphoma 2
BSA	Bovine serum albumin
CeO_2 NP	Cerium Oxide nanoparticles
ECL	Enhanced chemiluminiscence
eEF2	Eukaryotic elongation factor 2
eEF-2K	Eukaryotic elongation factor kinase
HSP	Heat shock proteins
JNK	c-Jun N- terminal kinase
LC3	Microtubule associated protein light chain 3
MAPK	Mitogen - activated protein kinase
NF-kB	Nuclear factor - kappaB
PCD	Programmed cell death
ROS	Reactive oxygen species
SEM	Standard Error Mean
SDS-PAGE	Sodium Dodecyl Sulfate-Polyacrylamide Gel Electrophoresis
TBS	Tris buffered saline
TBST	Tris buffered saline with 0.5% tween

LIST OF TABLES

LIST OF FIGURES

ABSTRACT

The growing application of cerium oxide nanoparticles (CeO_2 NP) in several industrial products is likely to be associated with increased risk of inhalation and exposure. How the inhalation of CeO_2 NP may affect cardiac structure and function has to our knowledge, not been examined. To examine whether inhalation of CeO_2 NP affects cardiac structure and function, male Sprague Dawley rats underwent a single intra tracheal instillation of nanoparticles (7 mg/kg body weight). Animals were sacrificed 1, 3, 14, and 28 days after instillation and protein isolates from the hearts were examined for the presence of oxidative stress, autophagy and apoptosis. Compared to 1 day saline controls, heart weights after instillation were decreased by 7.8 ± 1.9%, 12.2 ± 3.4%, 10.7 ± 3.2%, and 18.6 ± 3.9% at 1, 3, 14, and 28 days, respectively ($p<0.05$). Decreases in heart weight were associated with elevations in the expression of heat shock proteins (HSP) and NF-kB while the expression of AMPK-α was decreased suggesting the induction of oxidative stress subsequent to CeO_2 NP exposure. Further analysis demonstrated that the inhalation of the nanoparticles was also associated with elevations in the amount of Beclin-1 and LC3 which suggests that CeO_2 NP exposure can induce autophagy in the rat heart. Taken together, these data suggest that the inhalation of CeO_2 NP can cause increased cardiac oxidative stress and autophagy.

Key words: CeO_2 NP; oxidative stress; autophagy; apoptosis.

Chapter 1

Introduction

There is a great deal of interest in the effects that environmental pollutants and particulate matter may have on the development of respiratory and cardiovascular disease. While air born microscopic particles are a ubiquitous result of industrialization, the advent of nanotechnology and its rapid development has led to a concern related to the manufacturing and use of large quantities of nanoparticles (NP) (1). Many of the chemical and physical properties of nano-materials, such as a large surface to volume ratio and enhanced reactivity allow for different effects than that seen in their bulky counterparts. As such, the health effects of NP are attracting considerable concern from the public and governments worldwide (2).

One particular type NP of interest is that which is composed of cerium oxide (CeO_2). CeO_2 is the most abundant member of lanthanide series of metals. CeO_2 NP play a key role in technology and industrial applications for solar cells, fuel cells, gas sensors, oxygen pumps, and glass/ceramic applications (3). In addition, CeO_2 NPs have also been widely used in the automobile industries to reduce particulate matter emissions. Given its fluorite lattice structure and oxygen vacancies, CeO_2 NP can either give or take the oxygen atoms depending on the surrounding oxygen concentration (4). Recent work has also shown that the addition of cerium oxide to fuel reduces the nitric oxide and sulfur dioxide emissions, decreases fuel consumption and aids in the conversion of harmful carbon monoxide to carbon dioxide. These properties make cerium oxide NP an efficient catalytic converter for thermal applications such as natural gas combustion (4).

Recent studies have also suggested the CeO_2 NP may have potential for biomedical applications. CeO2 NP have been used to suppress the inflammatory processes in the myocardium and in the reduction of oxidative stress (5), to help protect neurons from oxidative toxicity (6), for the treatment of macular degeneration and other retinal diseases by inhibiting reactive oxygen species levels (7) and for protecting tissues from the damaging effects of radiation (8).

How CeO_2 NP may cause cellular toxicity is not well understood. Most of work done to date has been *in-vitro* using cultured cells (9-11). Based on previous studies, the toxicity of CeO_2 NP appears to vary with size, particle shape and degree of aggregation. Because of its widespread application as a polishing agent in the manufacturing sector it is likely that the most common route of exposure to CeO_2 NP will occur via inhalation. Although recent studies have shown that inhaled CeO_2 NP can cause lung damage and fibrosis, whether CeO_2 NP can exit the lungs after inhalation, and if able, whether CeO_2 NP are capable of damaging other organs and tissues is not well understood.

In the lung, exposure to CeO_2 NP is thought to be associated with increased oxidative stress, tissue fibrosis and evidence of increased endoplasmic reticulum stress (12). Whether CeO_2 NP exhibit similar effects in the heart, has to our knowledge, not been investigated.

Significance of the study

The growing application of CeO_2 NP in several industrial applications is likely to be associated with increased risk of exposure to these materials. A greater understanding of whether exposure to CeO_2 NP is toxic is needed to ensure worker safety. Thus far, the potential effects of inhaled CeO_2 NP on the heart are not well understood. This study is designed to specifically address this gap in our understanding.

Hypothesis

The primary objective of this study is to determine whether the inhalation of CeO_2 NP is associated with cardiac damage. We hypothesize that CeO_2 NP are capable of moving from the lung to the heart and that the presence of CeO_2 NP in the heart will be associated with indices of cellular stress. To test this hypothesis, two specific aims will be pursued:

Specific Aim 1: To determine if inhaled CeO_2 NP can induce oxidative stress in the rat heart.

Hypothesis: Inhaled CeO_2 NP will be associated with increased cardiac oxidative stress.

Specific Aim 2: To determine if inhaled CeO_2 NP can induce autophagy and/or apoptosis in the rat heart.

Hypothesis: Inhalation of CeO_2 NP will induce autophagy and/or apoptosis.

Chapter 2

A review of the literature pertinent to the present study will be discussed in this chapter. The following areas will be addressed: (i.) increasing importance of nanotechnology, (ii.) nanoceria applications, (iii.) toxic effects of CeO2 nanoparticles, (iv.) oxidative stress induced by cerium oxide nanoparticles, (v.) role of heat shock proteins (HSP) in oxidative stress, (vi.) AMPK alpha in oxidative stress, (vii.) autophagy in response to oxidative stress, and (viii.) eEF-2K role in autophagy.

Increasing importance of Nanotechnology

Nanotechnology is defined as technological applications of materials and assemblies at the nanometric scale (1-100 nm) (13). At the nanometer scale, the physical, chemical and biological properties of materials are fundamentally different from those of individual atoms, molecules and bulk materials (14). Nanomaterials exhibit a tremendous amount of potential for electronic, biomedical, pharmaceutical, cosmetic, energy, environmental, catalytic and material applications. The use of nanoparticles may be of significant benefit to many aspects of our lives, but the possible impact(s) that these materials may have on human health is not known. In addition to risks from use of the nanomedicine products, there are also concerns about the occupational and environmental risks associated with the manufacture and disposal of nano-drugs and nano-devices. As such, increasing our understanding of nanotoxicity is becoming a growing area of concern (13).

Nanoceria applications

Ceria exhibits two valance states (Ce^{+3} and Ce^{+4}). CeO_2 nanoparticles (CeO_2NP) are widely used in industrial applications as well as biomedical applications. Industrial uses includes solar cells, fuel cells, gas sensors, oxygen pumps, glass/ceramic applications and the automobile industry (3). The addition of cerium oxide to fuel acts to reduce particulate emissions like nitric oxide and sulfur dioxide while it also converts harmful carbon monoxide to carbon dioxide (4).

Cerium oxide nanoparticles have also been shown to act as free radical scavengers and may promote cell and organism longevity (15). Schubert *et al.,* demonstrated that CeO_2 nanoparticles are able to rescue HT22 cells from oxidative stress-induced cell death (1). Similarly, CeO_2 nanoparticles have also been shown to protect normal human breast cells from radiation-induced apoptotic cell death (16). In the heart, CeO_2 nanoparticles have been demonstrated to provide protection against cardiac dysfunction and remodeling induced by oxidative stress and inflammation, most likely due to causing a reduction of the inflammatory cytokines, TNF-alpha and IL-6 (5). Nanoceria have also been shown to exhibit super oxide dismutase (SOD) and catalase mimetic activity in a redox-state dependent manner (17). Other work has demonstrated that CeO_2 NP may also protect the neurons from oxidative damage (6), prevent macular degeneration (7) and that these particles may exhibit promise for protecting tissues from the damaging effects of radiation (8).

Toxic effects of CeO_2 nanoparticles

The inhalation of nanoparticles is increasingly recognized as a major cause of adverse health effects and may be associated with increased cardiovascular disease morbidity and mortality (18). The results of Gómez-Aracena *et al*., 2006 have suggested a relationship between chronic cerium exposure and increased risk of acute myocardial infarction (19). In certain geographic regions soil containing higher levels of cerium appears to be correlated with higher levels of cerium in serum and cardiac tissue of individuals with endomyocardial fibrosis (20-22).

Endocardial fibrosis has been shown by Kumar *et al*., 1995 after the administration of cerium chloride (1.3 mg/kg) into the tail vein of female Sprague-Dawley rats. These data were consistent with other work by Kumar *et al*., who reported that incubation of cardiac fibroblasts *in vitro* with 100 nM cerium increased RNA synthesis by 64% (Shivakumar *et al*., 1992). Taken together, these findings suggest that low levels of cerium exposure may act at the transcriptional level to stimulate collagen and non-collagen protein synthesis which may contribute to the accumulation of collagen in endocardial fibrosis.

Oxidative stress induced by cerium oxide nanoparticles

Oxidative stress is the imbalance between production of reactive oxygen and nitrogen species and the ability of a system to detoxify them. Reactive oxygen species (ROS) are a group of free radicals having unpaired electrons (23). ROS are highly reactive and can cause oxidative

damage to lipids, proteins and DNA (24). It is thought that the mitochondria are a major source of free radical generation. To counteract these adverse effects, cells utilize antioxidant enzymes such as superoxide dismutase, glutathione and catalase (25). An imbalance between the production and degradation of ROS results in ROS accumulation and further cell damage.

Until now, very little has been known about how nanoparticles may cause toxicity and the induction of oxidative stress which if unchecked can lead to apoptosis, cell cycle arrest and the inhibition of antioxidant enzymes. *In vivo* studies with aquatic species has showed that fullerenes can cause oxidative damage and a reduction in glutathione levels (26). Recent studies indicated the toxic effects of CeO_2 NP are mainly through induction of oxidative stress (3, 11). *In vitro* studies using A549 cells and *E. coli* treated with CeO_2 NP have shown elevations in cellular ROS, lipid peroxidation, cellular damage and reductions in cell viability (9, 27).

It has been postulated that one of the important upstream signaling mechanisms responsible for regulating oxidative stress are the mitogen-activated protein kinase (MAPK) cascades. There are three main groups of MAPK proteins: the extracellular signal-regulating kinase (ERK), p38 and c-Jun N-terminal kinase (JNK) (28). In 2008, Park *et al*., showed that while CeO_2 NP exposure did not alter total MAPK expression it was associated with increased p38-MAPK phosphorylation (3). Most of the studies involving ROS formation and MAP kinase signaling suggest that CeO_2 NP provoke oxidative stress (3, 11). Moreover, oxidative stress induced by the CeO_2 NP has been shown to cause 2-8 fold increases in cellular apoptosis (11). Although not fully understood, exposure to CeO_2 nanoparticles has also been observed to cause elevations in caspase-3 and chromatin condensation (3).

Oxidative stress and increased production of ROS after nutrient deprivation and ischemia-reperfusion are also associated with autophagy (29). Kirkland *et al*., showed that loss of mitochondrial inner membrane lipid cardiolipin causes increased apoptosis and autophagy, and that this process is mediated by increases in cellular free radicals (30).

Role of heat shock proteins (HSP) in oxidative stress

Increased production of heat shock proteins have been found to occur following cellular exposure to elevated temperatures, hypoxia, ischemia, heavy metal intoxication and increased cellular ROS levels (31). Heat shock proteins help stabilize improperly folded proteins and protect them from degradation (32). Hsp27 also known as HspB1 will interact with several cytoskeleton components like actin, microtubules and intermediate metabolites (33). The microfilament network is an early target of oxidative stress and is protected from degradation by Hsp 27 (34). Hsp27 also has a protective role following exposure to heavy metals (35). Hsp27 also has a role in controlling apoptosis and the regulation of caspase expression (36). Other work has shown that Hsp27 may also play a protective role in dilated cardiomyopathy and ischemia-reperfusion injury (37). It is thought that HSP27 over expression increases NF-kB activity which may function to suppress apoptosis (38). According to Kim H, et al, inhibition of Hsp60 will suppress autophagy under conditions of increased oxidative stress (39). It appears that Hsp60 exhibits anti-apoptotic effects by the suppression of caspase activity (40).

Role of AMPK alpha in oxidative stress

The adenosine mono phosphate-activated protein kinase (AMPK) is an enzyme which is a key regulator of cellular energy balance (41). AMP-activated protein kinase is a serine/threonine kinase consisting of α, β and γ subunits. Among these, the α subunit consists of two isoforms α_1 and α_2. It is thought that the α subunit is catalytic in nature while the β and γ function to maintain the stability of the complex. Recent studies have suggested that suppression of AMPK activity is linked with oxidative stress (42) and the inflammatory response (43). Other data has shown that inhibition of AMPK activity can ameliorate oxidative damage (44) and inflammation (45). Similarly, AMPK has been shown to play a protective role during oxidative stress while reductions of AMPK activity are associated with increases in NAD(P)H oxidase activity and ROS production. The AMPK activator, Metformin, has been shown to reduce oxidative stress in aortic endothelial cells (46). Likewise, the activation of AMPK through AICAR (5-aminoimidazole-4-carboxamide-1-beta-D-ribofuranoside) inhibits the ROS-induced apoptosis in endothelial cells (47). AMPK may also have an effect on NF-kB activation as the activity of this pathway can be suppressed by activated AMPK which leads to decreased expression of NAD(P)H oxidase (42). According to Chao Liu et al., AMPK α activation promotes cell survival through increasing NF-kB mediated expression and suppression of apoptosis (48).

Autophagy in response to oxidative stress

Programmed cell death (PCD) has been described as an important protective mechanism. It is thought that there are two different forms of PCD; apoptosis and autophagy

(49). Autophagy is a lysosomal dependent protein degradation pathway, which involves the degradation of pathogens and damaged organelles allowing the reuse of nutrients under nutrient deprived conditions. If excessive, autophagy can be detrimental to cells and lead to cell death. Recent studies have shown that apoptosis and autophagy, can act simultaneously in the cell death processes (50).

During autophagy, a membrane is formed around the cytoplasmic contents of interest. Once formed, this structure binds with lysosomes through and the components are subjected to enzymatic reactions within the lysosomes. Hydrolases play a key role in this enzymatic degradation. The resulting molecules will be released into cytoplasm for further recycling (51).

In the last decade approximately 30 autophagy related genes (*ATG* genes) have been identified in yeast cells and 16 homologous genes have been identified in mammalian cells (52). Among these genes, the Beclin-1 and LC3 (microtubule associated protein light chain 3) are thought to play a key role in mammalian autophagy. Beclin-1 (the mammalian homolog of yeast Atg6 gene), is required for autophagic vesicle formation (53). Beclin 1 is identified as an important point of convergence between apoptosis and autophagy as it is associated with anti apoptotic Bcl2 like proteins (54).

LC3, a mammalian homolog of yeast Atg8 and is considered a reliable marker of autophagy as it represents the amount of autophagosomes at that particular time. Conversion of LC3I to LC3II is indicative of autophagic activity. Because the half-life of LC3II is short, autophagosomes are transient structures. LC3II levels are representative of autophagic activity at any one moment in time (55). During autophagy, the cytoplasmic form (LC3I) is processed and recruited to the autophagosomes, where LC3II is generated by site specific proteolysis near

the C-terminus. The hallmark of autophagic activation is thus the formation of cellular autophagosome punctae containing LC3II, while autophagic activity is measured biochemically as the amount of LC3II that accumulates in the absence or presence of lysosomal activity. It is thought that exposure to some nanomaterials is associated with the autophagy dysregulation in autophagy leading to an increase in the number of autophagosomes (56).

eEF-2K role in autophagy

eEF2 (Eukaryotic elongation factor) is required for mRNA translation elongation (57, 58). The phosphorylation of eEF2 at Thr-56 inactivates its inhibitory effect on mRNA translation. The phosphorylation of eEF2 is mediated by eEF-2K, when it is phosphorylated at Thr-366 (59). One of the upstream regulators of eEF-2K is transforming growth factor (TGFβ). Falguni Das and colleagues showed that TGF-β treatment of mesengeal cells is associated with cellular hypertrophy and that this process occurred via the activation of eEF2 (57).

Both eEF2 and eEF2K are thought to play a role in the induction of autophagy. According to Wu *et al*., down regulation of eEF-2K expression in gliobastoma cells following treatment with siRNA was associated with diminished autophagy and the down regulation of the autophagy mediator LC3 (58). Other work, using T98G gliobastoma cells that were engineered to over express eEF-2K has shown that elevations in eEF-2 were found to be associated with increased autophagy (60). It is thought that eEF-2K plays a key role in crosstalk between autophagy and apoptosis as the inhibition of eEF-2K activity in tumor cells appears to suppress autophagy and promote apoptosis (61, 62).

Summary

The toxic effects of CeO_2 NP are thought to occur via the generation of ROS. If excessive, elevations in ROS can lead to changes in the degree of HSP, NF-kB, eEF-2K, AMPK, Beclin-1 and LC3 activity which can cause the induction of autophagy and apoptosis. How CeO_2 NP may affect the intact heart is not well understood.

Chapter 3

To be submitted to the Journal of Nanotoxicology

Abstract

The growing application of cerium oxide nanoparticles (CeO_2 NP) in several industrial products is likely to be associated with increased risk of inhalation and exposure. How the inhalation of CeO_2 NP may affect cardiac structure and function has to our knowledge, not been examined. To examine whether inhalation of CeO_2 NP affects cardiac structure and function, male Sprague Dawley rats underwent a single intra tracheal instillation of nanoparticles (7 mg/kg body weight). Animals were sacrificed 1, 3, 14, and 28 days after instillation and protein isolates from the hearts were examined for the presence of oxidative stress, autophagy and apoptosis. Compared to 1 day saline controls, heart weights after instillation were decreased by 7.8 ± 1.9%, 12.2 ± 3.4%, 10.7 ± 3.2%, and 18.6 ± 3.9% at 1, 3, 14, and 28 days, respectively ($p<0.05$). Decreases in heart weight were associated with elevations in the expression of heat shock proteins (HSP) and NF-kB while the expression of AMPK-α was decreased suggesting the induction of oxidative stress subsequent to CeO_2 NP exposure. Further analysis demonstrated that the inhalation of the nanoparticles was also associated with elevations in the amount of Beclin-1 and LC3 which suggests that CeO_2 NP exposure can induce autophagy in the rat heart. Taken together, these data suggest that the inhalation of CeO_2 NP can cause increased cardiac oxidative stress and autophagy.

Key words: CeO_2 NP; oxidative stress; autophagy; apoptosis.

Introduction

The ever increasing use of nanomaterials for industrial applications has led to concerns regarding the potential effects these materials may have on cellular life and the environment. When compared to bulk materials, nanoparticles exhibit an increased surface area / weight ratio which can leads to increased reactivity and different physico-chemical properties (2). Cerium dioxide nanoparticles (CeO_2 NP) are widely used in the solar cells, fuel cells, gas sensors, and polishing industries. CeO_2 NP are also used as catalysts and as fuel additives where they function to reduce the emission of sulfur dioxide and nitric oxide from fuel and help to covert carbon monoxide to carbon dioxide. Recent studies have also suggested the CeO_2 NP may have potential for biomedical applications as antioxidant. CeO_2 NP have been used to suppress the inflammatory processes in the myocardium and in the reduction of oxidative stress (5), to help protect neurons from oxidative toxicity (6), for the treatment of macular degeneration and other retinal diseases by inhibiting reactive oxygen species levels (7) and for protecting tissues from the damaging effects of radiation (8). Although very promising for in vivo application, whether CeO_2 NP exhibit toxic effects to cells and tissues is not well understood. Thus far, most of work done to date has been *in-vitro* using cultured cells (9-11). Although recent studies have shown that inhaled CeO_2 NP can cause lung damage and fibrosis, whether CeO_2 NP can exit the lungs after inhalation, and if able, whether CeO_2 NP are capable of damaging other organs and tissues is not well understood.

In the lung, exposure to CeO_2 NP is thought to be associated with increased oxidative stress, tissue fibrosis and evidence of endoplasmic reticulum stress (12). Whether CeO_2 NP exhibit similar effects in the heart, has to our knowledge, not been investigated. Interestingly,

recent data has demonstrated that the inhalation of carbon nanotubes may be associated with the deposition of nanotubes elsewhere in the body (63). On the basis of these data, we hypothesized that CeO_2 NP inhalation could lead to the translocation of CeO_2 NP from the heart to the lung. In addition, we also hypothesized that the presence of CeO_2 NP in the heart would be associated with evidence of oxidative stress. Taken together, our data suggest that the inhalation of CeO_2 NP is associated with increased oxidative stress and autophagy in hearts of male Sprague Dawley rats.

Materials and Methods

Particle characterization

CeO_2 nanoparticles, 10% weight in water (average diameter at ~20 nm), were obtained from Sigma-Aldrich (St Louis, MO). For installation normal saline was used as vehicle. Diluted particle suspensions were filtered, sputter coated, and examined with a Hitachi Model S-4800 Field Emission scanning electron microscope (Schaumburg, IL, USA) at 5 and 20 kV or placed on a formvar-coated copper grid to dry and imaged with a JEOL 1220 transmission electron microscope (Tokyo, Japan).

Animals

All procedures were performed in accordance with the Marshall University Institutional Animal Care and Use Committee (IACUC) guidelines, using the criteria outlined by the Assessment and Accreditation of Laboratory Animal Care (AAALAC). 5 weeks old 150-174 g weighing Specific pathogen-free male Sprague-Dawley (Hla: SD-CVF) rats were purchased from Hilltop Lab Animals, Inc. (Scottdale, PA, USA). Rats were housed two per cage in an AAALAC approved vivarium with a 12-h light–dark cycle, temperature maintained at 22 ± 2 °C, and fed *ad libitum*. All animals were allowed to acclimatize for 2 weeks before initiation of any treatment or procedures. All animals were examined for precipitous weight loss, failure to thrive or unexpected gait. Periodic weight measurements were taken throughout the duration of the study.

Materials

Beclin-1 (#3738), LC3B (#2775), Phospho AMPK-α $^{Thr\ 172}$(#2535), AMPK-α (#2532), Bax (#2772), Bcl-2(# 2870), Phospho eEF-2k $^{Ser\ 366}$(#3691), eEF-2k(#3692), Hsp60(D307)(#4870) Mouse IgG, and Rabbit IgG antibodies were purchased from cell signaling technology(Beverly, MA). NF-kB p50 (E-10)(sc-8414), Hsp27 (M-20)(sc-1049), HeLa whole cell lysate (sc-2200) and L6+ IGF lysate(sc-24727) were purchased from Santa Cruz Biotechnology(Santa Cruz, CA). Enhance chemiluminescence (ECL) western blotting detection reagent was purchased from Amersham Biosciences (Piscataway, NJ). Restore western blot stripping buffer was obtained from Pierce (Rockford, IL). Dihydroethidium (5mM standard solution in DMSO) was purchased from molecular probes (Invitrogen, OR). TUNEL assay kit was purchased from Roche diagnostics corporation (Mannheim, Germany). All other chemicals were purchased from Sigma Aldrich (St.Louis,MO) or Fisher Scientific (Hanover, IL).

Rationale for Dose at the rate of 7mg/kg B.wt

The dose i.e 7mg/kg B.wt was determined by an estimation of the amount of CeO_2 that can be inhaled from diesel exhaust over an 8 hr period is 0.09 µg/kg (HEI, 2001). The total lung burden after 40 years of occupational exposure can be estimated as the following as 0.09 ug/kg/d X 5 d/week X 52 week/year X 40 years = 936 µg/kg and the safety factor conversion from humans to rodents is 10. So it is reasonable to examine the systemic toxicological effects of CeO_2 nanoparticles exposure from 1.0 mg/kg to 7.0mg/kg. Previous studies show that it took 28 days to observe histological alterations in the lungs (64). So we investigated the effects of CeO_2 NP on the heart for 28 days.

Instillation of CeO_2 nanoparticles

After acclimatization, animals were divided randomly into 8 groups (n=6 per group). Each group of the animals were anesthetized with sodium methohexital (35 mg/kg, i.p.) and placed on an inclined restraint board before instillation with 0.3 ml of saline suspension of CeO_2 nanoparticles at a dose rate of 7mg/kg B.wt. All animals were humanely treated and were monitored for any potential suffering. Rats were euthanized and collected the tissues at 1, 3, 14, and 28 days post exposure of CeO_2 nanoparticles and control groups with normal saline according to the Guidelines for the Care and Use of Laboratory Animals.

Tissue collection

Rats were anesthetized with a ketamine–xylazine (4:1) cocktail (50 mg/kg, I/P) and supplemented as necessary for reflexive response before tissue collections. The heart was removed and placed in Krebs–Ringer bicarbonate buffer (KRB) containing; 118 mM NaCl, 4.7 mM KCl, 2.5 mM CaCl2, 1.2 mM KH2PO4, 1.2 mM MgSO4, 24.2 mM NaHCO3, and 10 mM α-D-glucose (pH 7.4) equilibrated with 5%CO_2/95%O_2 and maintained at 37^0 C. Blood and other tissue materials are removed from the Isolated hearts, then weighed, and immediately snap frozen in liquid nitrogen.

TUNEL staining

Heart tissues (control, day 1, 3 and 14 post exposure) were sectioned (8 µm) using an IEC Microtome cryostat and collected on poly-lysine coated slides. DNA fragmentation was determined by TdT-mediated dUTP nick end labeling (TUNEL) as outlined by the manufacturer

(In Situ Cell Death Detection Kit, Roche Diagnostics, Mannheim, Germany). Briefly, sections were fixed with 4% paraformaldehyde, washed with PBS (pH 7.4), and then permeabilized with 0.1% sodium citrate and 0.1% Triton-X. Nuclei were counter stained using DAPI (VECTASHIELD Hard Set Mounting Medium, Vector Laboratories, Burlingame, CA). Heart cross sections were visualized by epifluorescence using an Olympus fluorescence microscope (Melville, NY) fitted with 20X and 40X objectives and images were recorded digitally using a CCD camera (Olympus, Melville, NY). The number of TUNEL positive nuclei was counted in three randomly selected regions in each slide. Three different animals were counted from each group. Tissue sections treated with DNase I to induce DNA fragmentation were used as a positive control.

DHE staining

Hydroethidine (HE) staining was used to detect superoxide radical generation. Hydroethidine is cell permeable and in the presence of free oxygen radicals becomes oxidized to ethidium bromide which intercalates with DNA (65). Heart tissue sections (8 µm) were incubated with 5 µM dihydroethidium stain (Invitrogen, OR) at 37^0 C for 30 min. After thorough washing with PBS (pH 7.4) mounting with DAPI (VECTASHIELD Hard Set Mounting Medium, Vector Laboratories, Burlingame, CA) sections were visualized for epifluorescence using an Olympus fluorescence microscope (Melville, NY). Images were recorded digitally using a CCD camera (Olympus, Melville, NY). Images from four randomly selected regions from each slide were collected for observation. Data was collected from at least three animals at each time point. Images were quantified by AlphaView image analysis software (Alpha Innotech, San Leandro,CA).

Immunoblotting analysis

Portions of individual heart tissues (100-150mg) were homogenized in buffer (T-PER, 8 mL/g tissue; Pierce, Rockford, IL) containing protease (P8340, Sigma-Aldrich, Inc., St. Louis, MO, USA) and phosphatase inhibitors (P5726, Sigma-Aldrich, Inc., St. Louis, MO). Tissue homogenates were sonicated (3 x 30 sec cycles at 50 W) and the supernatant collected by centrifuging (12,000g x 5 min at 4 °C). Protein concentrations were determined in triplicate using the 660 nm assay method (Thermo Scientific, Rockford, IL). Equal concentrations of the protein samples were prepared from each of the individual samples by adding equal quantities of sample buffer and adjusting the protein concentration with the TPER lysis buffer. Samples were boiled in a Laemmli sample buffer (Sigma-Aldrich, Inc., St. Louis, MO) for 5 min. Forty micrograms of total protein for each sample was separated on a 10% PAGEr Gold Precast gel (Lonza, Rockland, ME) and then transferred to nitrocellulose membranes (Amersham, NJ). Gels were stained with a RAPID Stain protein stain reagent (G-Biosciences, St. Louis, MO, USA) to verify transfer efficiency. Membranes were stained with Ponceau S and the amount of protein was quantified by densitometry to confirm successful transfer of proteins and equal loading of lanes. Membranes were blocked with 5% milk in Tris Buffered Saline (TBS) containing 0.05% Tween-20 (TBST) for 1 h and then incubated with primary antibody overnight at 4C. After washing with 1%TBST, the membranes were incubated with the corresponding secondary antibodies conjugating with horseradish peroxidase (HRP) (anti-rabbit (#7074) or anti-mouse (#7076), Cell Signaling Technology, Danvers, MA) for 1 h at room temperature. Protein bands were visualized following reaction with ECL reagent (Amersham ECL Western Blotting reagent

NJ). Target protein levels were quantified by AlphaView image analysis software (Alpha Innotech, San Leandro, CA).

Data Analysis

Results are presented as mean ± SEM. Data were analyzed using the Sigma Plot 11.0 statistical program. One-way analysis of variance was performed for overall comparisons, while the Student–Newman–Keuls post hoc test used to determine differences between groups. Values of $P<0.05$ were considered to be statistically significant.

Results

CeO_2 NP inhalation decreases heart weight

Compared to control animals, CeO_2 NP exposure did not affect feed intake and weight gain (Table 2). Compared to age matched control animals, heart weights were 7.8 ± 1.9%, 12.2 ± 3.4%, 10.7 ± 3.2%, and 18.6 ± 3.9% less at 1, 3, 14 and 28 days, respectively (*P<0.05*) (Table 1).

CeO_2 NP inhalation increases superoxide levels but not TUNEL reactivity

The quantification of O_2^- was determined semi-quantitatively by assessing the oxidation of hydroethidine to ethidium bromide. Compared to control animals, the amount of ethidium fluorescence was 34.4 ± 12.3%, 78.6 ± 6.4%, and 72.1 ± 8.6% higher at 1, 3, and 14 days post exposure, respectively (*P<0.05*)(Figure 1). Compared to control animals, CeO_2 inhalation did not increase the number of TUNEL reactive cells at any time (Data not shown).

CeO_2 NP inhalation increases HSP27 and HSP60 expression

The abundance of HSP27 and HSP60 were determined from protein isolates obtained from each of the different groups. Compared to control animals, the amount of HSP27 was 27.1 ± 3.8%, 33.7 ± 4.6%, 36.7 ± 5.1%, and 17.4 ± 6.2% higher at 1, 3, 14 and 28 days after CeO_2 instillation, respectively (*P<0.05*) (Figure 2). Similarly, HSP60 expression was 9.9 ± 5.8%, 41.4 ± 2.8%, 58.2 ± 7.0%, and 48.7 ± 4.8% higher after 1, 3, 14, and 28 days, respectively (*P<0.05*) (Figure 3).

CeO_2 NP inhalation alters AMPK-α phosphorylation and NF-kB expression

Compared to control animals, CeO_2 NP inhalation decreased the amount of phosphorylated AMPK-α by 23.5 ± 1.8% and 27.2 ± 1.2% at 1 and 3 days post instillation (*P<0.05*). Conversely, CeO_2 NP inhalation, appeared to increase AMPK-α phosphorylation by 15.5 ± 5.1% and 20.6 ± 5.7% at days 14 and 28 post exposure (*P<0.05*) (Figure 5). Compared to that observed in the control animals, NF-kB p50 protein levels in CeO_2 exposed animals were 42.8 ± 9.5% and 25.4 ± 7.5% higher at days 14 and 28 day, respectively (*P<0.05*) (Figure 4).

CeO_2 NP inhalation increases the ratio of Bax/Bcl-2 protein one day after exposure

Compared to control animals, the ratio of Bax / Bcl-2 protein was 42.4 ± 6.9% higher in CeO_2 exposed animals at day 1 (*P<0.05*). Conversely, the ratio of Bax / Bcl-2 was 26.4 ± 3.3% lower at day 14 post exposure (*P<0.05*) (Figure 6).

CeO_2 NP inhalation appears to be associated with increased cardiac autophagy

Compared to control animals, the expression of Beclin-1 was 21.0 ± 2.2%, 18.9 ± 1.9%, and 13.9 ± 2.3% higher 1, 3 and 14 days post exposure, respectively (*P<0.05*) (Figure 7). Similarly, LC3-II protein content was 26.1 ± 1.9 and 57.4 ± 11.7 higher 3 and 28 days post exposure (*P<0.05*) (Figure 8). Compared to control animals, with CeO_2 inhalation, the phosphorylation of eEF-2K was 18.1 ± 3.5%, 19.9 ± 5.2%, and 19.5 ± 4.5% higher at days 1, 3, and 14 day post exposure (*P<0.05*) (Figure 9).

Discussion

CeO_2 NP are widely used in a number of industrial applications and in the fuel cell, solar cell and polishing industries. It is thought that CeO_2 NP may also exhibit potential medical use given their ability to act as a free radical scavenger. Recent *in vitro* studies have suggested that CeO_2 NP may also have toxic effects given their proclivity to increase the generation of reactive oxygen species and decease intracellular glutathione levels in cells at higher concentrations (3). Whether CeO_2 NP are toxic to cardiac cells *in vivo,* has to our knowledge, not been investigated. The primary finding of this study is that CeO_2 NP inhalation appears to be associated with evidence of increased oxidative stress in the Sprague Dawley rat heart (Figure 1). This increase in oxidative stress was found to be associated with alterations in the amount of autophagic (Beclin-1, LC3-II), transcriptional (NF-kB) and heat shock (HSP27, HSP 60) protein expression (Figures 2- 9).

How nanoparticles may cause cellular toxicity is not well understood. Recent data has suggested that nanoparticles exposure is oftentimes associated with increases in cellular

reactive oxygen species (3, 9, 11, 26, 27). We observed similar findings in the present study (Figure 1). On the basis of previous reports showing that HSP expression are regulated, at least in part, by oxidative stress levels (31, 34), we next examined if cerium oxide inhalation was associated with increases in the amount of cardiac heat shock protein HSP27 and HSP60. It is thought that HSP function in various capacities to minimize cellular damage (32). As an example, the Hsp27 has been shown to exhibit anti-apoptotic activity (36) while other work has also shown that Hsp27 over expression can increase the activity of NF-kB (38). Compared to control animals, our data suggest that CeO_2 NP inhalation is associated with elevations in both Hsp27 and Hsp60 levels (Figure 2 and 3). Like that observed for the HSPs, the expression of NF-kB was also elevated after inhalation CeO_2 NP (Figure 4). Similar to the HSPs, elevations in NF-kB have also been shown to induced by increases in cellular ROS (66) where they, like the HSPs may function to protect the cell from apoptosis (37). Whether these elevations in HSP and NF-kB protein expression are a direct result of the increased oxidative stress associated with the inhalation of CeO_2 NP is currently unclear.

Interestingly, we found that the amount of phosphorylated AMPK was lower in the animals that were sacrificed after 1- and 3 days of CeO_2 inhalation and higher, compared to control, in animals that were sacrificed after 14- and 28 days of CeO_2 inhalation (Figure 5). It is thought that the AMPK functions as an energy sensor and that diminished AMPK phosphorylation can be caused by increases in oxidative stress or by cellular inflammation (42, 43). Some studies indicated increased AMPK phosphorylation will cause increased expression of NF-kB protein and further suppression of apoptosis (48). Our results indicated increased

expression of AMPK in 14 and 28 days post exposure. The other pathways influenced the increased expression of NF-kB protein is unclear and further investigation is needed.

Two downstream outcomes of increased oxidative stress are the induction of programmed cell death and autophagy. It is thought that the transition to cellular apoptosis is controlled, at least in part, by the ratio of the pro-apoptotic Bax protein and the anti-apoptotic Bcl-2 proteins (67). Herein, we found an elevation in the ratio of Bax / Bcl-2 one day after CeO_2 exposure suggesting that cerium oxide inhalation may be associated with increases in cardiac apoptosis (Figure 6). Whether this latter possibility actually occurs will require further investigation.

Similar to that seen with apoptosis, previous work has suggested that autophagy proteins may play a protective role in maintaining overall tissue function (51). To examine if cerium oxide inhalation is associated with cardiac authophagy we next examined the tissue levels of the autophagy regulators beclin-1 and LC3-II levels (53, 54). Our data demonstrated increases in amount of beclin-1 at 1, 3, and 14 days post exposure (Figure 7). Consistent with these data, we also found increases in LC3-II protein levels at days 3 and 28 day (Figure 8). Similar to what we observed for beclin-1, and consistent with the induction of autophagy (60), eEF-2K protein levels were found to be elevated at 1, 3 and 14 days post exposure (Figure 9). Elevated expression of these three autophagy related proteins clearly indicated there is increased autophagy in the absence of apoptosis which suggest that this process is a pro-survival mechanism rather than one associated with cell death.

Taken together, our data suggest that intra tracheal instillation of CeO_2 NP in male Sprague Dawley rats is associated with increased oxidative stress in the heart, elevations in the

amount of Hsp27, Hsp60, and NF-kB protein expression. These alterations were, in turn, also associated with evidence of cardiac autophagy (Figure 10). Given these findings, future work to further examine how cerium oxide inhalation may affect cardiac function may be warranted.

APPENDIX

TABLES AND FIGURES

Table 1. Effect of CeO2 inhalation on rat body and heart weight.

	Groups				
	Control	**1day CeO_2 NP**	**3 day CeO_2 NP**	**14 day CeO_2 NP**	**28 day CeO_2 NP**
Body weight, g	319.6±6.4	319.6±6.2	331.6±9.8	332.3±8.6	411.3±11.9
Heart weight, g	1.1±0.03	1.2±0.11	1.0±0.02	1.1±0.03	1.3±0.04
Heart wt / B.wt	3.64±0.02	3.36±0.02*	3.2±0.03*	3.25±0.03*	2.96±0.04*

(Mean±SEM), * significantly different than 1 day saline control ($p<0.05$)

Table 2. Effect of CeO2 inhalation on rat feed intake and body weight gain per week

	Groups			
	14 day Control	**14 day CeO_2 NP**	**28 day Control**	**28 day CeO_2 NP**
Feed intake (g)	179.1±10.0	196.1±15.5	192.3±4.5	189.2±4.1
Body weight gain (g)	21±1.1	18.6±2.1	26.2±1.4	23.2±1.5

(Mean±SEM)

Figure 1

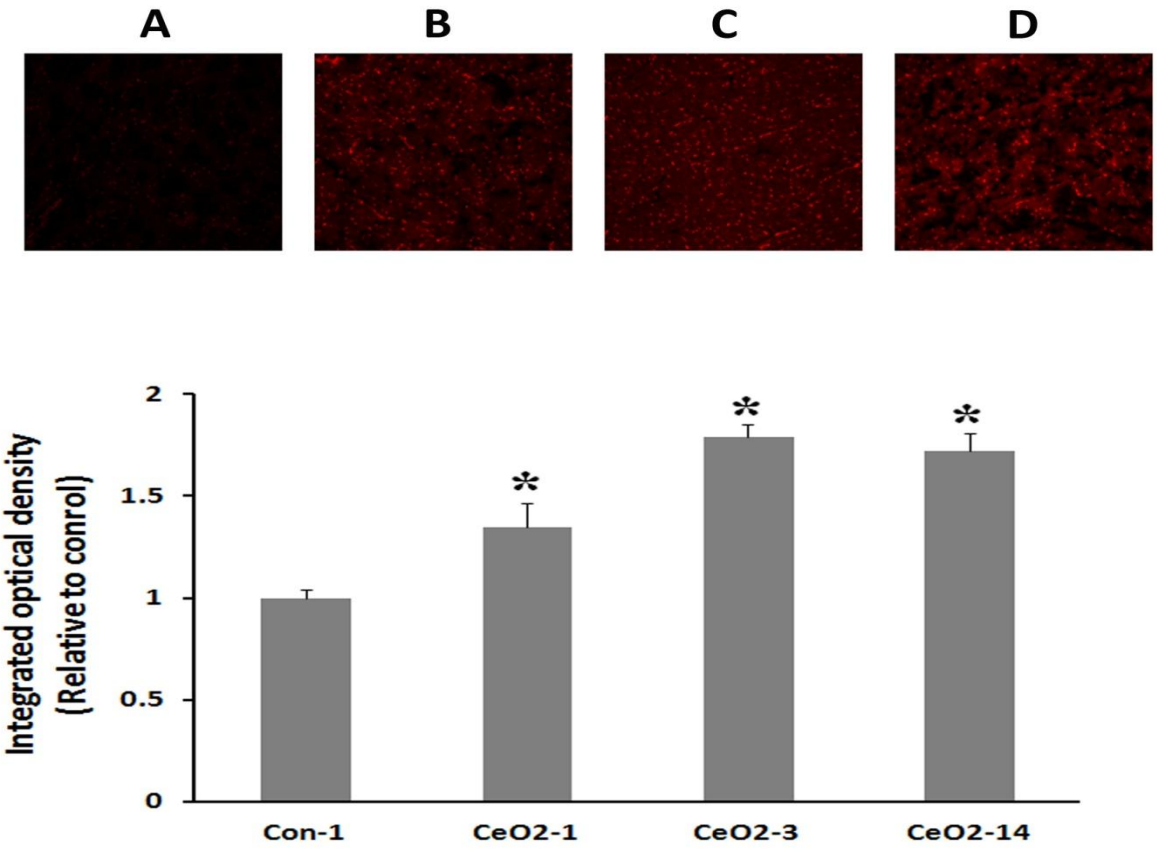

Figure 1. CeO_2 NP instillation increases cardiac superoxide levels.

Cardiac ROS determined by intensity of fluorescent ethidium bromide – stained nuclei. Results are expressed as a means ± SEM. * significantly different from 1 day control ($p<0.05$). n=4 hearts per group.

Figure 2

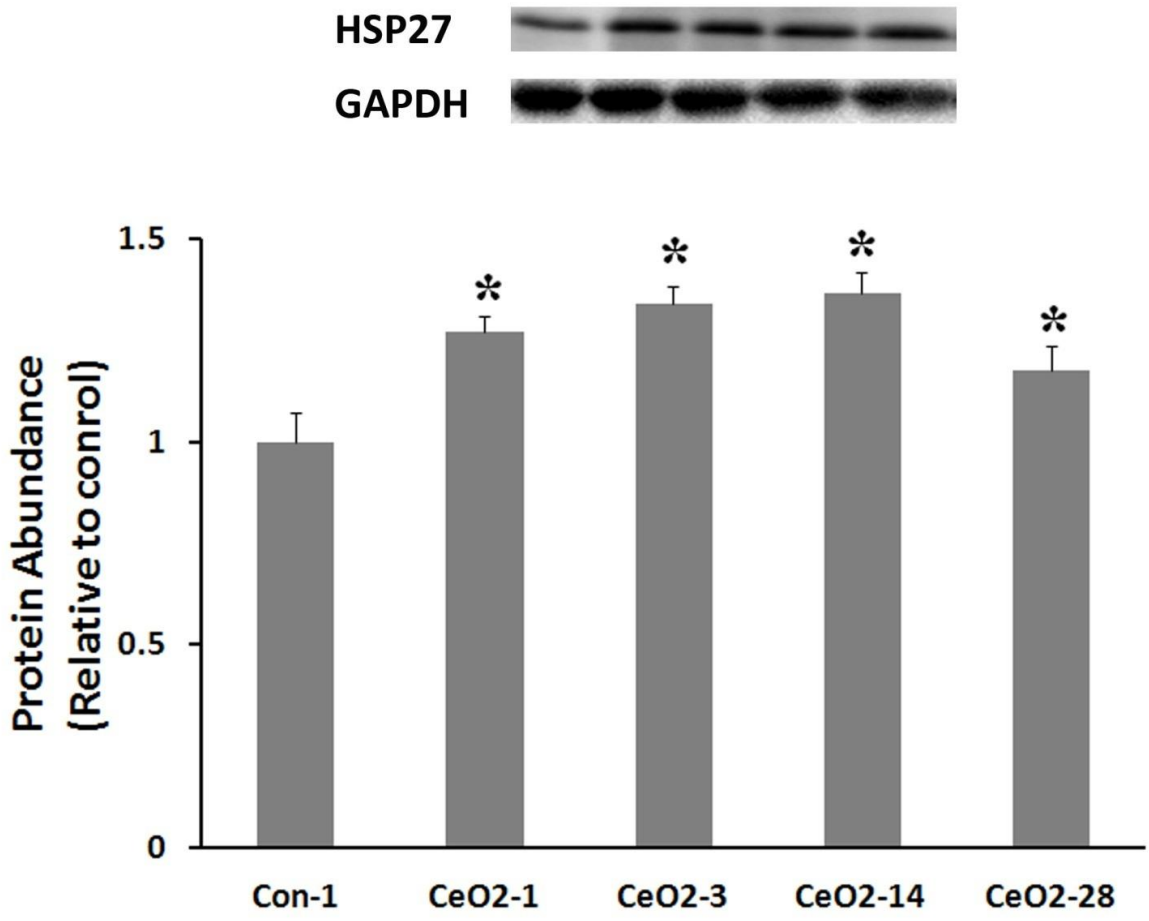

Figure 2. Expression of Hsp27 is altered with CeO_2 NP instillation.

Protein samples from 1 day control, 1 day, 3 day, 14 day, and 28 day CeO_2 NP were analyzed by immunoblotting. Results are expressed as a means ± SEM. * significantly different from 1 day control ($p<0.05$).

Figure 3

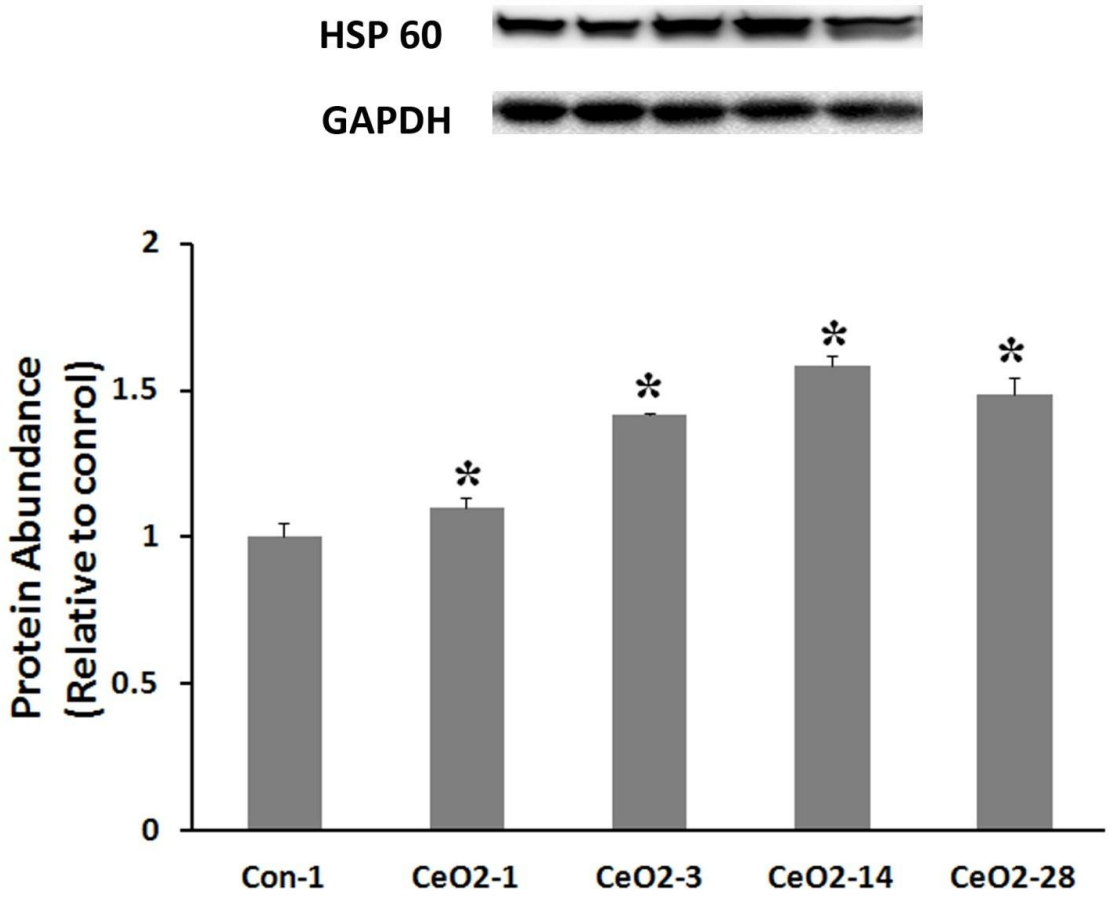

Figure 3. Expression of Hsp60 is altered with CeO_2 NP instillation.

Protein samples from 1 day control, 1 day, 3 day, 14 day, and 28 day CeO_2 NP were analyzed by immunoblotting. Results are expressed as a means ± SEM. * significantly different from 1 day control ($p<0.05$).

Figure 4

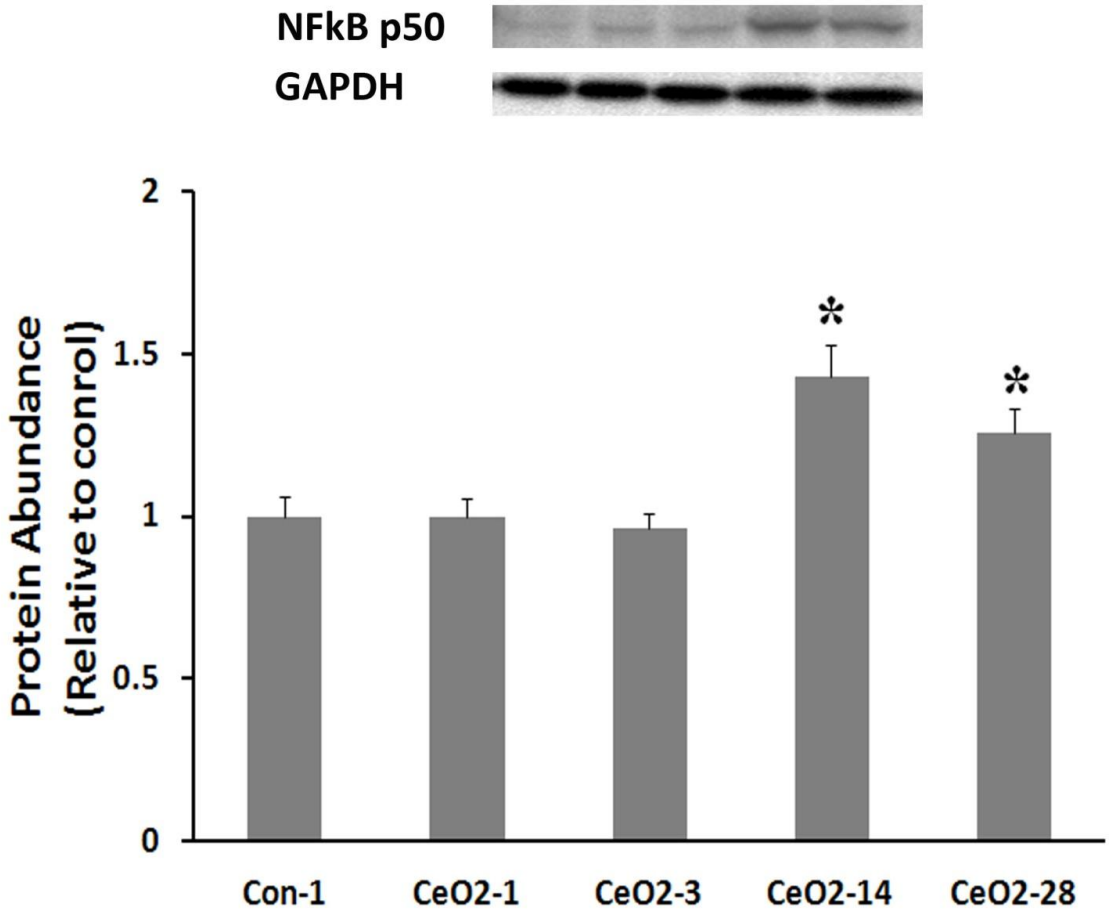

Figure 4. Expression of NF-kB p50 is altered with CeO_2 NP instillation.

Protein samples from 1 day control, 1 day, 3 day, 14 day, and 28 day CeO_2 NP were analyzed by immunoblotting. Results are expressed as a means ± SEM. * significantly different from 1 day control ($p<0.05$).

Figure 5

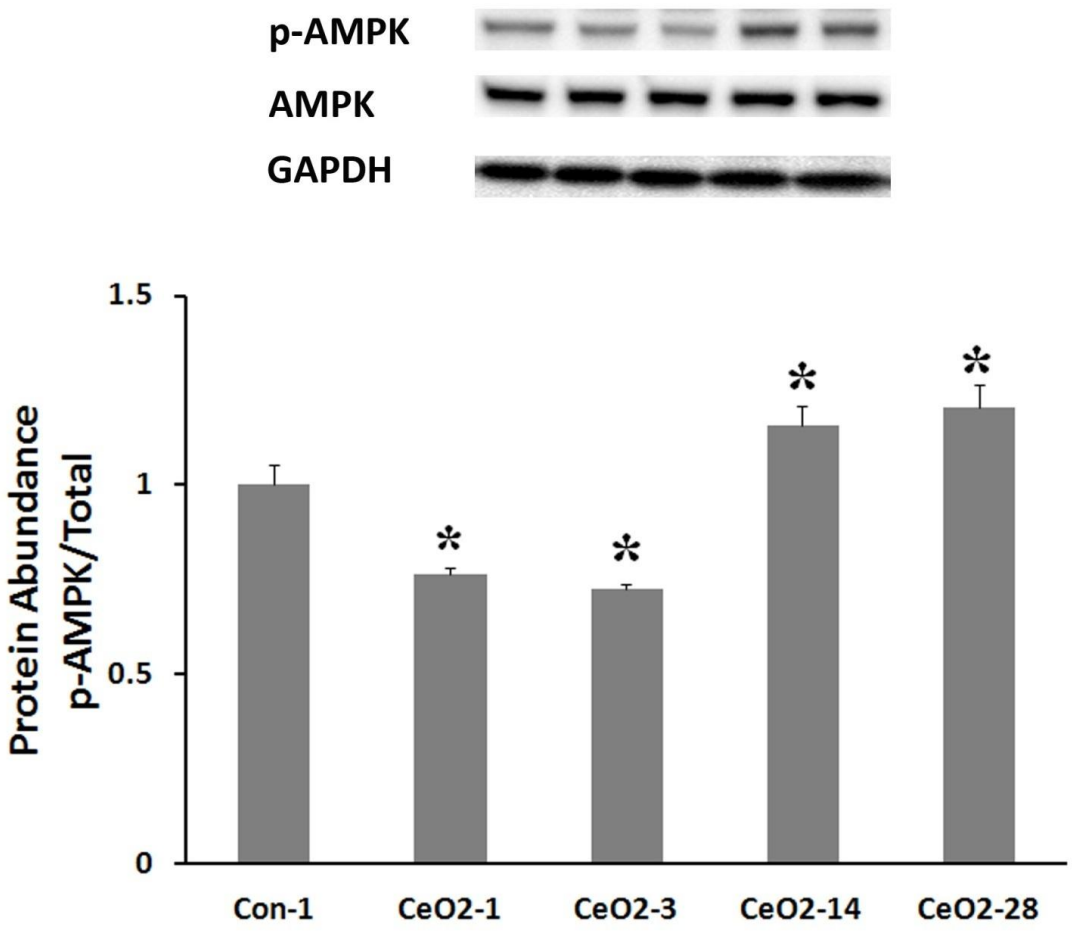

Figure 5. Phosphorylation of AMPK α is altered with CeO_2 NP instillation.

Protein samples from 1 day control, 1 day, 3 day, 14 day, and 28 day CeO_2 NP were analyzed by immunoblotting. Results are expressed as a means ± SEM. * significantly different from 1 day control ($p<0.05$).

Figure 6

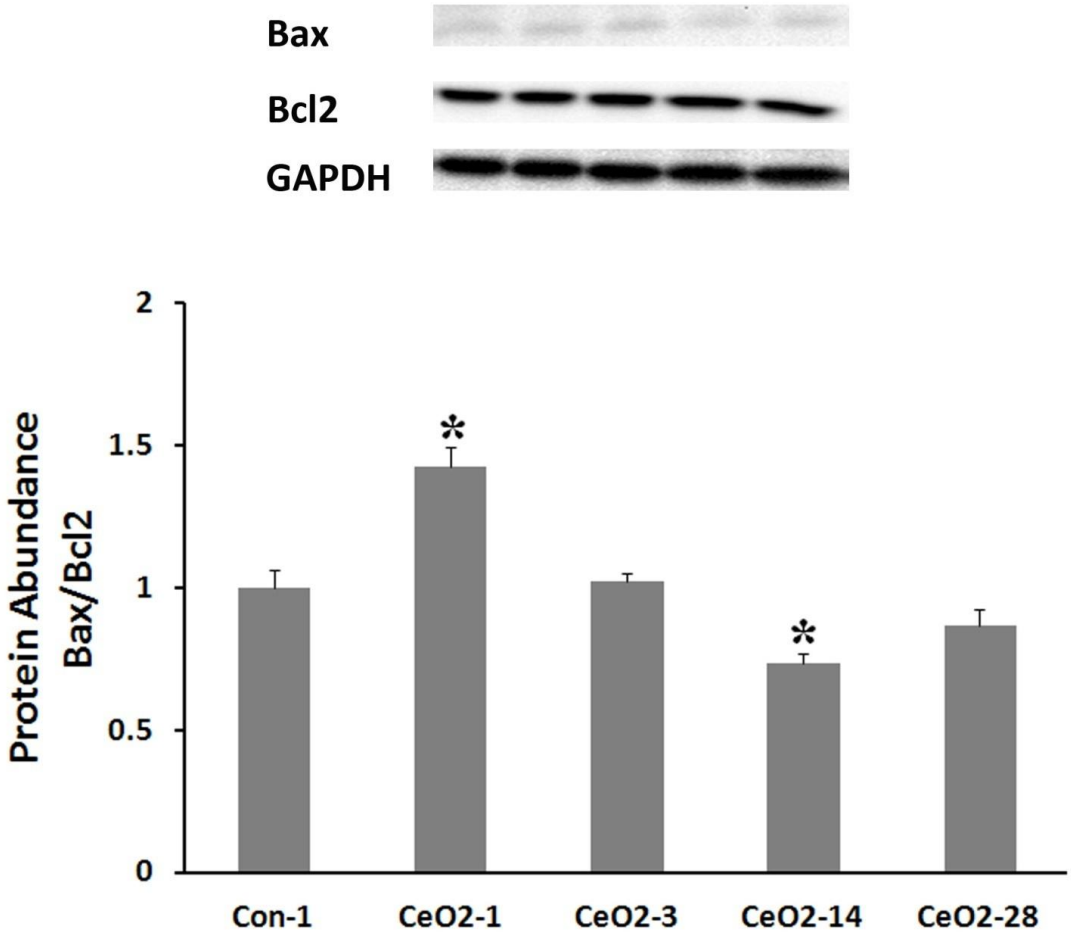

Figure 6. Expression of Bax/Bcl-2 is altered with CeO_2 NP instillation.

Protein samples from 1 day control, 1 day, 3 day, 14 day, and 28 day CeO_2 NP were analyzed by immunoblotting. Results are expressed as a means ± SEM. * significantly different from 1 day control ($p<0.05$).

Figure 7

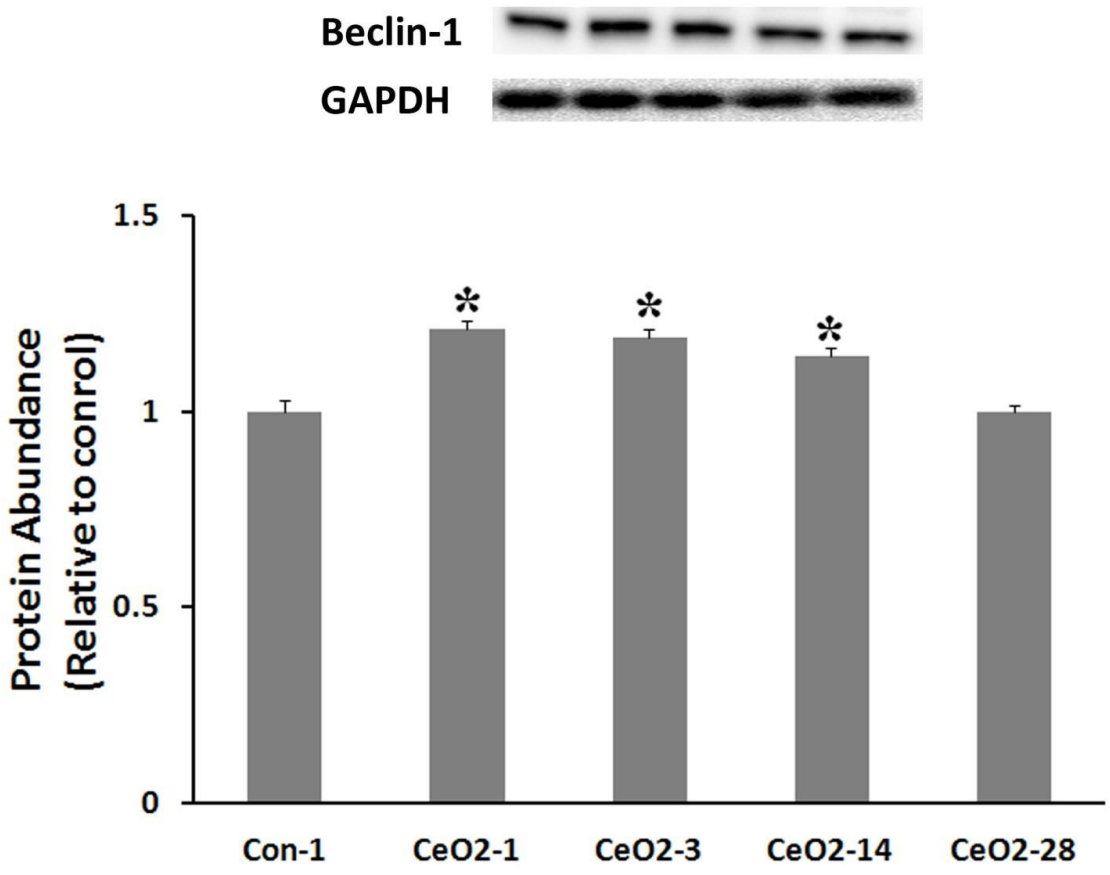

Figure 7. Expression of Beclin-1 is altered with CeO_2 NP instillation.

Protein samples from 1 day control, 1 day, 3 day, 14 day, and 28 day CeO_2 NP were analyzed by immunoblotting. Results are expressed as a means ± SEM. * significantly different from 1 day control ($p<0.05$).

Figure 8

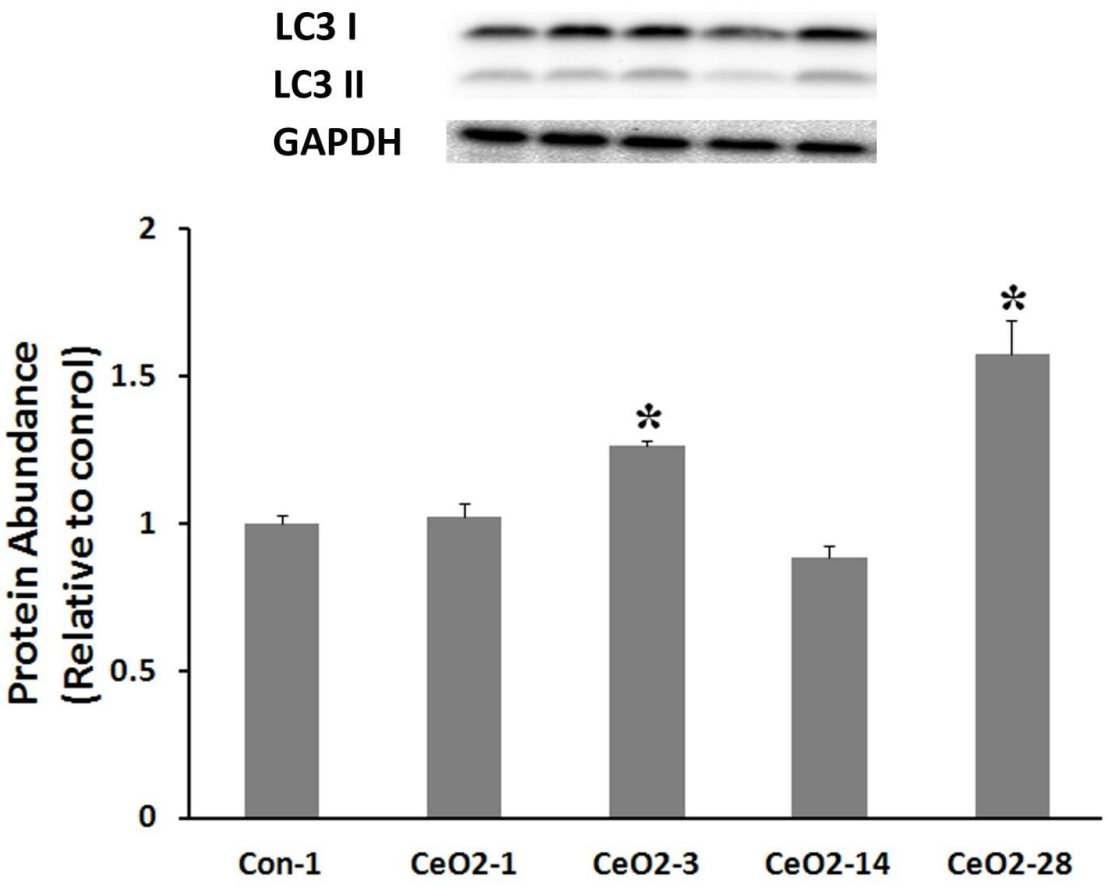

Figure 8. Conversion of LC3 is altered with CeO_2 NP instillation.

Protein samples from 1 day control, 1 day, 3 day, 14 day, and 28 day CeO_2 NP were analyzed by immunoblotting. Results are expressed as a means ± SEM. * significantly different from 1 day control($p<0.05$).

Figure 9

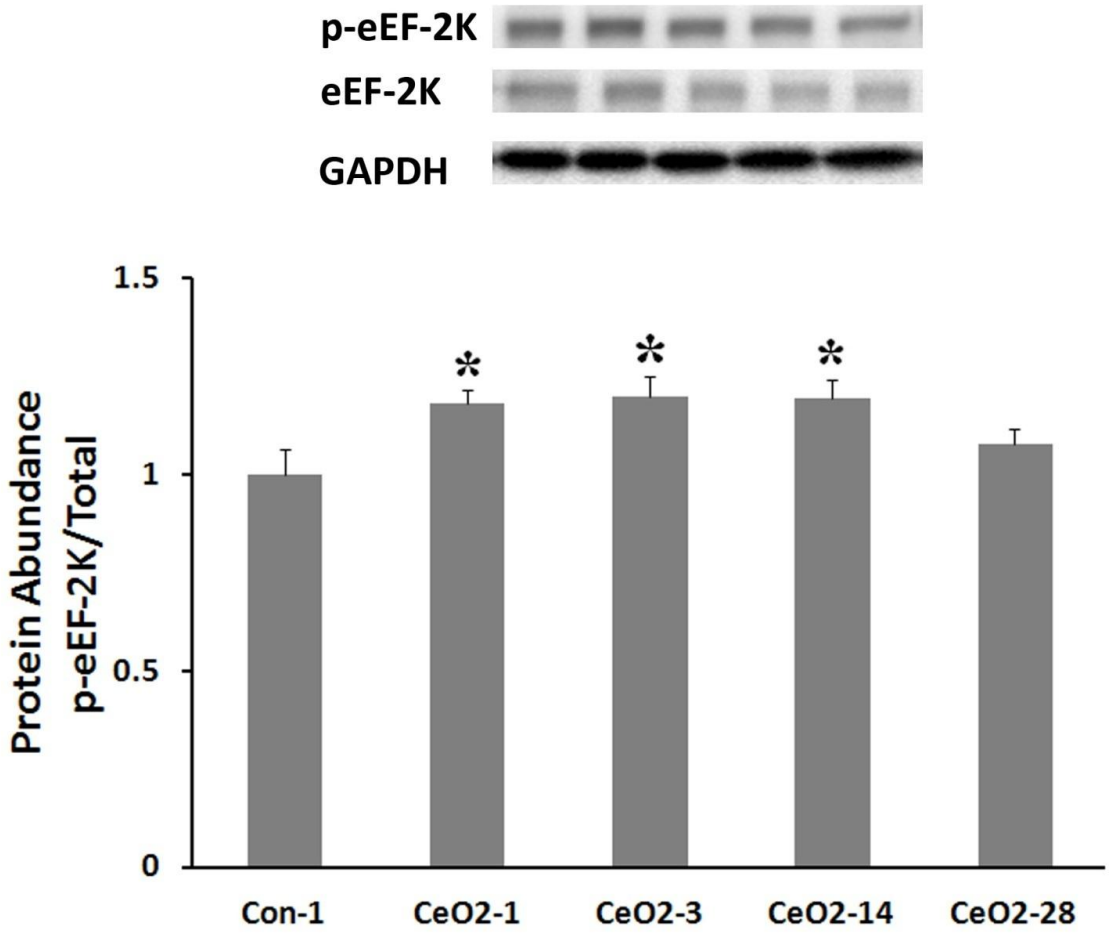

Figure 9. Phosphorylation of eEF-2K is altered with CeO_2 NP instillation.

Protein samples from 1 day control, 1 day, 3 day, 14 day, and 28 day CeO_2 NP were analyzed by immunoblotting. Results are expressed as a means ± SEM. * significantly different from 1 day control ($p<0.05$).

Figure 10

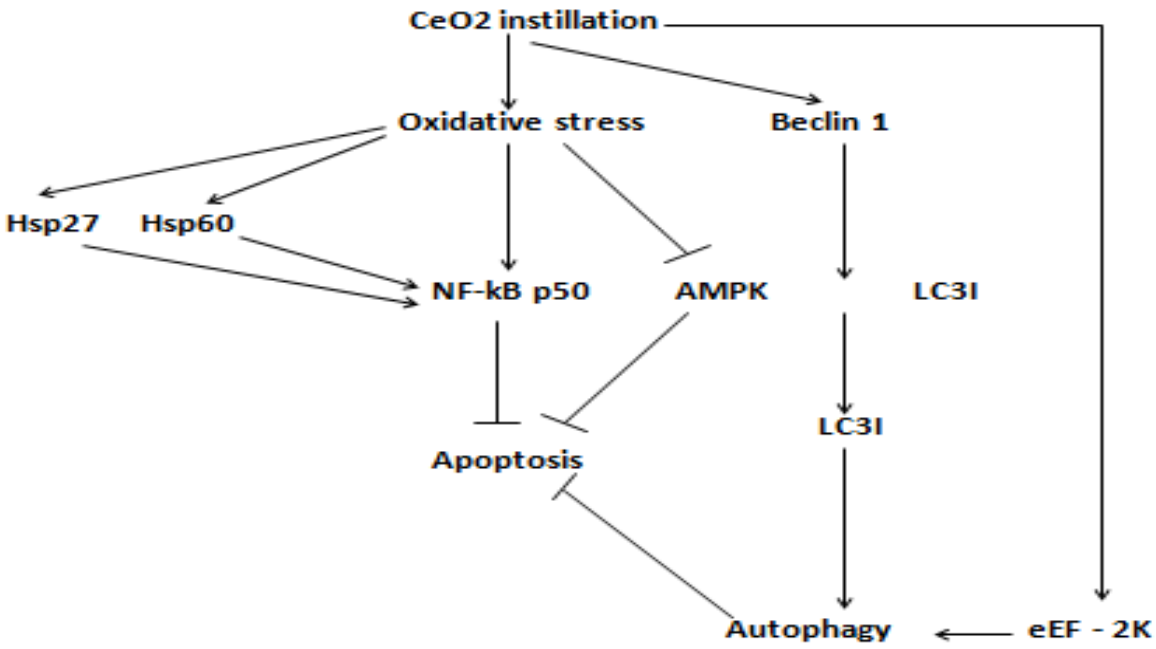

Figure 10. Effects of CeO_2 NP inhalation on the Sprague Dawley rat heart.

Chapter 4

Conclusions

Cerium oxide is widely used in several industrial applications and may also exhibit potential use for the treatment of various biomedical conditions. Here we examine the potential toxicological effects of inhaled CeO_2 NP on the heart. Our data suggest that the inhalation of CeO_2 NP is associated with increased cardiac oxidative stress and evidence of cardiac autophagy.

Specifically, our data suggest the following:

1. Inhalation of CeO_2 NPs is associated with diminished heart mass.
2. Inhalation of CeO_2 NPs is associated with evidence of increased cardiac superoxide levels.
3. Inhalation of CeO_2 NPs is associated with increased expression of heat shock proteins in the heart.
4. Inhalation of CeO_2 NPs is associated with evidence of increased cardiac autophagy in the absence of cardiac apoptosis.

Future directions

Our results suggest that the inhalation of CeO_2 NP poses a potential toxicity risk to the heart. The time course of this study was relatively short in that it only last four weeks. As such, it is not clear if the effects we observed at one month post exposure represent long term changes or not. On the basis of these data, it may be useful for future studies to investigate the

long term effects of inhalation exposure to CeO_2 NP. In addition, it is not clear if CeO_2 NP accumulate over time in the heart. This lack in our understanding could also be addressed. Similarly it is unclear if the changes we see at the biochemical level are associated with changes in cardiac structure and function. To address this, future studies could also be done using echocardiography to see if CeO_2 exposure is associated with changes in cardiac performance.

References

1. Schubert D, Dargusch R, Raitano J, & Chan SW (2006) Cerium and yttrium oxide nanoparticles are neuroprotective. (Translated from eng) *Biochem Biophys Res Commun* 342(1):86-91 (in eng).
2. Liu Y*, et al.* (2009) Potential health impact on mice after nasal instillation of nano-sized copper particles and their translocation in mice. (Translated from eng) *J Nanosci Nanotechnol* 9(11):6335-6343 (in eng).
3. Park EJ, Choi J, Park YK, & Park K (2008) Oxidative stress induced by cerium oxide nanoparticles in cultured BEAS-2B cells. (Translated from eng) *Toxicology* 245(1-2):90-100 (in eng).
4. Bumajdad A, Eastoe J, & Mathew A (2009) Cerium oxide nanoparticles prepared in self-assembled systems. (Translated from eng) *Adv Colloid Interface Sci* 147-148:56-66 (in eng).
5. Niu J, Azfer A, Rogers LM, Wang X, & Kolattukudy PE (2007) Cardioprotective effects of cerium oxide nanoparticles in a transgenic murine model of cardiomyopathy. (Translated from eng) *Cardiovasc Res* 73(3):549-559 (in eng).
6. Das M*, et al.* (2007) Auto-catalytic ceria nanoparticles offer neuroprotection to adult rat spinal cord neurons. (Translated from eng) *Biomaterials* 28(10):1918-1925 (in eng).
7. Chen J, Patil S, Seal S, & McGinnis JF (2006) Rare earth nanoparticles prevent retinal degeneration induced by intracellular peroxides. (Translated from eng) *Nat Nanotechnol* 1(2):142-150 (in eng).
8. Colon J*, et al.* (2009) Protection from radiation-induced pneumonitis using cerium oxide nanoparticles. (Translated from eng) *Nanomedicine* 5(2):225-231 (in eng).
9. Lin W, Huang YW, Zhou XD, & Ma Y (2006) Toxicity of cerium oxide nanoparticles in human lung cancer cells. (Translated from eng) *Int J Toxicol* 25(6):451-457 (in eng).
10. Gojova A*, et al.* (2009) Effect of cerium oxide nanoparticles on inflammation in vascular endothelial cells. (Translated from eng) *Inhal Toxicol* 21 Suppl 1:123-130 (in eng).
11. Eom HJ & Choi J (2009) Oxidative stress of CeO2 nanoparticles via p38-Nrf-2 signaling pathway in human bronchial epithelial cell, Beas-2B. (Translated from eng) *Toxicol Lett* 187(2):77-83 (in eng).
12. Younce CW & Kolattukudy PE (2010) MCP-1 causes cardiomyoblast death via autophagy resulting from ER stress caused by oxidative stress generated by inducing a novel zinc-finger protein, MCPIP. (Translated from eng) *Biochem J* 426(1):43-53 (in eng).
13. Teli MK, Mutalik S, & Rajanikant GK (2010) Nanotechnology and nanomedicine: going small means aiming big. (Translated from eng) *Curr Pharm Des* 16(16):1882-1892 (in eng).
14. Nowack B & Bucheli TD (2007) Occurrence, behavior and effects of nanoparticles in the environment. (Translated from eng) *Environ Pollut* 150(1):5-22 (in eng).
15. Singh N, Cohen CA, & Rzigalinski BA (2007) Treatment of neurodegenerative disorders with radical nanomedicine. (Translated from eng) *Ann N Y Acad Sci* 1122:219-230 (in eng).
16. Tarnuzzer RW, Colon J, Patil S, & Seal S (2005) Vacancy engineered ceria nanostructures for protection from radiation-induced cellular damage. (Translated from eng) *Nano Lett* 5(12):2573-2577 (in eng).
17. Pirmohamed T*, et al.* (2010) Nanoceria exhibit redox state-dependent catalase mimetic activity. (Translated from eng) *Chem Commun (Camb)* 46(16):2736-2738 (in eng).
18. Mills NL*, et al.* (2009) Adverse cardiovascular effects of air pollution. (Translated from eng) *Nat Clin Pract Cardiovasc Med* 6(1):36-44 (in eng).

19. Gomez-Aracena J*, et al.* (2006) Toenail cerium levels and risk of a first acute myocardial infarction: the EURAMIC and heavy metals study. (Translated from eng) *Chemosphere* 64(1):112-120 (in eng).
20. Eapen JT (1998) Elevated levels of cerium in tubers from regions endemic for endomyocardial fibrosis (EMF). (Translated from eng) *Bull Environ Contam Toxicol* 60(1):168-170 (in eng).
21. Kutty VR, Abraham S, & Kartha CC (1996) Geographical distribution of endomyocardial fibrosis in south Kerala. (Translated from eng) *Int J Epidemiol* 25(6):1202-1207 (in eng).
22. Eapen JT, Kartha CC, Rathinam K, & Valiathan MS (1996) Levels of cerium in the tissues of rats fed a magnesium-restricted and cerium-adulterated diet. (Translated from eng) *Bull Environ Contam Toxicol* 56(2):178-182 (in eng).
23. Riley PA (1994) Free radicals in biology: oxidative stress and the effects of ionizing radiation. (Translated from eng) *Int J Radiat Biol* 65(1):27-33 (in eng).
24. Holler N*, et al.* (2000) Fas triggers an alternative, caspase-8-independent cell death pathway using the kinase RIP as effector molecule. (Translated from eng) *Nat Immunol* 1(6):489-495 (in eng).
25. Mates JM & Sanchez-Jimenez F (1999) Antioxidant enzymes and their implications in pathophysiologic processes. *Front Biosci* 4:D339-345.
26. Oberdorster E (2004) Manufactured nanomaterials (fullerenes, C60) induce oxidative stress in the brain of juvenile largemouth bass. (Translated from eng) *Environ Health Perspect* 112(10):1058-1062 (in eng).
27. Thill A*, et al.* (2006) Cytotoxicity of CeO2 nanoparticles for Escherichia coli. Physico-chemical insight of the cytotoxicity mechanism. (Translated from eng) *Environ Sci Technol* 40(19):6151-6156 (in eng).
28. Kyriakis JM & Avruch J (2001) Mammalian mitogen-activated protein kinase signal transduction pathways activated by stress and inflammation. *Physiol Rev* 81(2):807-869.
29. Wu HH, Hsiao TY, Chien CT, & Lai MK (2009) Ischemic conditioning by short periods of reperfusion attenuates renal ischemia/reperfusion induced apoptosis and autophagy in the rat. (Translated from eng) *J Biomed Sci* 16:19 (in eng).
30. Kirkland RA, Adibhatla RM, Hatcher JF, & Franklin JL (2002) Loss of cardiolipin and mitochondria during programmed neuronal death: evidence of a role for lipid peroxidation and autophagy. (Translated from eng) *Neuroscience* 115(2):587-602 (in eng).
31. Mymrikov EV, Seit-Nebi AS, & Gusev NB (2011) Large potentials of small heat shock proteins. (Translated from eng) *Physiol Rev* 91(4):1123-1159 (in eng).
32. Vos MJ, Hageman J, Carra S, & Kampinga HH (2008) Structural and functional diversities between members of the human HSPB, HSPH, HSPA, and DNAJ chaperone families. (Translated from eng) *Biochemistry* 47(27):7001-7011 (in eng).
33. Landry J & Huot J (1995) Modulation of actin dynamics during stress and physiological stimulation by a signaling pathway involving p38 MAP kinase and heat-shock protein 27. (Translated from eng) *Biochem Cell Biol* 73(9-10):703-707 (in eng).
34. Huot J, Houle F, Spitz DR, & Landry J (1996) HSP27 phosphorylation-mediated resistance against actin fragmentation and cell death induced by oxidative stress. (Translated from eng) *Cancer Res* 56(2):273-279 (in eng).
35. Wu W & Welsh MJ (1996) Expression of the 25-kDa heat-shock protein (HSP27) correlates with resistance to the toxicity of cadmium chloride, mercuric chloride, cis-platinum(II)-diammine dichloride, or sodium arsenite in mouse embryonic stem cells transfected with sense or antisense HSP27 cDNA. (Translated from eng) *Toxicol Appl Pharmacol* 141(1):330-339 (in eng).

36. Concannon CG, Orrenius S, & Samali A (2001) Hsp27 inhibits cytochrome c-mediated caspase activation by sequestering both pro-caspase-3 and cytochrome c. (Translated from eng) *Gene Expr* 9(4-5):195-201 (in eng).
37. Tucker NR & Shelden EA (2009) Hsp27 associates with the titin filament system in heat-shocked zebrafish cardiomyocytes. (Translated from eng) *Exp Cell Res* 315(18):3176-3186 (in eng).
38. Parcellier A*, et al.* (2003) HSP27 is a ubiquitin-binding protein involved in I-kappaBalpha proteasomal degradation. (Translated from eng) *Mol Cell Biol* 23(16):5790-5802 (in eng).
39. Kim H*, et al.* (2009) Activation of autophagy during glutamate-induced HT22 cell death. (Translated from eng) *Biochem Biophys Res Commun* 388(2):339-344 (in eng).
40. Campanella C*, et al.* (2008) Upon oxidative stress, the antiapoptotic Hsp60/procaspase-3 complex persists in mucoepidermoid carcinoma cells. (Translated from eng) *Eur J Histochem* 52(4):221-228 (in eng).
41. Turdi S*, et al.* (2010) AMP-activated protein kinase deficiency exacerbates aging-induced myocardial contractile dysfunction. (Translated from eng) *Aging Cell* 9(4):592-606 (in eng).
42. Wang S*, et al.* (2010) AMPKalpha2 deletion causes aberrant expression and activation of NAD(P)H oxidase and consequent endothelial dysfunction in vivo: role of 26S proteasomes. (Translated from eng) *Circ Res* 106(6):1117-1128 (in eng).
43. Ko HJ*, et al.* (2009) Nutrient stress activates inflammation and reduces glucose metabolism by suppressing AMP-activated protein kinase in the heart. (Translated from eng) *Diabetes* 58(11):2536-2546 (in eng).
44. Ceolotto G*, et al.* (2007) Rosiglitazone reduces glucose-induced oxidative stress mediated by NAD(P)H oxidase via AMPK-dependent mechanism. (Translated from eng) *Arterioscler Thromb Vasc Biol* 27(12):2627-2633 (in eng).
45. Jeong HW*, et al.* (2009) Berberine suppresses proinflammatory responses through AMPK activation in macrophages. (Translated from eng) *Am J Physiol Endocrinol Metab* 296(4):E955-964 (in eng).
46. Ouslimani N*, et al.* (2005) Metformin decreases intracellular production of reactive oxygen species in aortic endothelial cells. (Translated from eng) *Metabolism* 54(6):829-834 (in eng).
47. Kim JE*, et al.* (2008) AMP-activated protein kinase activation by 5-aminoimidazole-4-carboxamide-1-beta-D-ribofuranoside (AICAR) inhibits palmitate-induced endothelial cell apoptosis through reactive oxygen species suppression. (Translated from eng) *J Pharmacol Sci* 106(3):394-403 (in eng).
48. Liu C, Liang B, Wang Q, Wu J, & Zou MH (2010) Activation of AMP-activated protein kinase alpha1 alleviates endothelial cell apoptosis by increasing the expression of anti-apoptotic proteins Bcl-2 and survivin. (Translated from eng) *J Biol Chem* 285(20):15346-15355 (in eng).
49. Shimizu S*, et al.* (2004) Role of Bcl-2 family proteins in a non-apoptotic programmed cell death dependent on autophagy genes. (Translated from eng) *Nat Cell Biol* 6(12):1221-1228 (in eng).
50. Pattingre S*, et al.* (2005) Bcl-2 antiapoptotic proteins inhibit Beclin 1-dependent autophagy. (Translated from eng) *Cell* 122(6):927-939 (in eng).
51. Xie Z & Klionsky DJ (2007) Autophagosome formation: core machinery and adaptations. (Translated from eng) *Nat Cell Biol* 9(10):1102-1109 (in eng).
52. Klionsky DJ*, et al.* (2003) A unified nomenclature for yeast autophagy-related genes. (Translated from eng) *Dev Cell* 5(4):539-545 (in eng).
53. Qu X*, et al.* (2003) Promotion of tumorigenesis by heterozygous disruption of the beclin 1 autophagy gene. (Translated from eng) *J Clin Invest* 112(12):1809-1820 (in eng).
54. Liang XH*, et al.* (1998) Protection against fatal Sindbis virus encephalitis by beclin, a novel Bcl-2-interacting protein. (Translated from eng) *J Virol* 72(11):8586-8596 (in eng).

55. Mizushima N (2009) Methods for monitoring autophagy using GFP-LC3 transgenic mice. (Translated from eng) *Methods Enzymol* 452:13-23 (in eng).
56. Zabirnyk O, Yezhelyev M, & Seleverstov O (2007) Nanoparticles as a novel class of autophagy activators. (Translated from eng) *Autophagy* 3(3):278-281 (in eng).
57. Das F, Ghosh-Choudhury N, Kasinath BS, & Choudhury GG (2010) TGFbeta enforces activation of eukaryotic elongation factor-2 (eEF2) via inactivation of eEF2 kinase by p90 ribosomal S6 kinase (p90Rsk) to induce mesangial cell hypertrophy. (Translated from eng) *FEBS Lett* 584(19):4268-4272 (in eng).
58. Wu H, Yang JM, Jin S, Zhang H, & Hait WN (2006) Elongation factor-2 kinase regulates autophagy in human glioblastoma cells. (Translated from eng) *Cancer Res* 66(6):3015-3023 (in eng).
59. Browne GJ & Proud CG (2002) Regulation of peptide-chain elongation in mammalian cells. (Translated from eng) *Eur J Biochem* 269(22):5360-5368 (in eng).
60. Hait WN, Wu H, Jin S, & Yang JM (2006) Elongation factor-2 kinase: its role in protein synthesis and autophagy. (Translated from eng) *Autophagy* 2(4):294-296 (in eng).
61. Cheng Y, Yan L, Ren X, & Yang JM (2011) eEF-2 kinase, another meddler in the "yin and yang" of Akt-mediated cell fate? (Translated from eng) *Autophagy* 7(6):660-661 (in eng).
62. Cheng Y*, et al.* (2011) eEF-2 kinase dictates cross-talk between autophagy and apoptosis induced by Akt Inhibition, thereby modulating cytotoxicity of novel Akt inhibitor MK-2206. (Translated from eng) *Cancer Res* 71(7):2654-2663 (in eng).
63. Wang H*, et al.* (2004) Biodistribution of carbon single-wall carbon nanotubes in mice. (Translated from eng) *J Nanosci Nanotechnol* 4(8):1019-1024 (in eng).
64. Ma JY*, et al.* (2011) Cerium oxide nanoparticle-induced pulmonary inflammation and alveolar macrophage functional change in rats. (Translated from eng) *Nanotoxicology* 5(3):312-325 (in eng).
65. Rothe G, Emmendorffer A, Oser A, Roesler J, & Valet G (1991) Flow cytometric measurement of the respiratory burst activity of phagocytes using dihydrorhodamine 123. *J Immunol Methods* 138(1):133-135.
66. Li N & Karin M (1999) Is NF-kappaB the sensor of oxidative stress? (Translated from eng) *FASEB J* 13(10):1137-1143 (in eng).
67. Oltvai ZN, Milliman CL, & Korsmeyer SJ (1993) Bcl-2 heterodimerizes in vivo with a conserved homolog, Bax, that accelerates programmed cell death. (Translated from eng) *Cell* 74(4):609-619 (in eng).